A linear sampling method for recovering a clamped cavity in a thin plate

Purdue Graduate Research Day

General Ozochiawaeze

Department of Mathematics
Purdue University

December 15, 2024

Overview

Inverse Shape Problem

- Send a wave and observe the reflected wave by an unknown obstacle
- **Question:** What information about the obstacle can one extract from the observed wave?
- **Type of waves:** *flexural waves in elastic plates* (biharmonic plate equation)
- **Applications:** nondestructive testing and designing devices for remote sensing, energy harvesting, and vibration isolation.

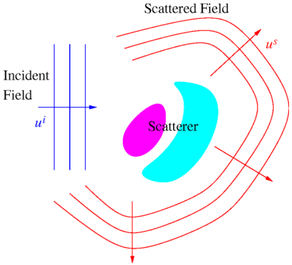

Model Equation for Thin Plate Bending

Model of out-of-plane displacement in a thin elastic plate

$$\boxed{\mathcal{D}\Delta^2 W + \rho h \frac{\partial^2 W}{\partial t^2} = 0}$$

- $\mathcal{D} := \frac{Eh^3}{12(1-\nu^2)}$: flexural rigidity
- $E > 0$: Young's modulus
- $\nu \in [0, \frac{1}{2})$: Poisson's ratio
- h: thickness
- ρ: density of material

Time-Harmonic Dependency: $W(x,t) = \mathrm{Re}\{u(x)e^{-i\omega t}\}$

Time-Harmonic Biharmonic Plate Equation

$$\boxed{\Delta^2 u - \kappa^4 u = 0, \quad \kappa^2 = \sqrt{\frac{\rho h \omega}{\mathcal{D}}} : \text{ wave number}}$$

Direct and Inverse Scattering of Biharmonic Waves

Problem (The Direct Clamped Cavity Scattering Problem)

We consider the time-harmonic biharmonic scattering problem

1. $D \subset \mathbb{R}^2$ *is a clamped (fixed) cavity with* $\partial D \in C^\infty(\mathbb{R}^2)$
2. *The cavity receives illumination from the incident plane wave* $u^i(x) = \exp(i\kappa x \cdot d)$

The total field $u = u^i + u^s \in H^2_{loc}(\mathbb{R}^2)$ *satisfies, with* $r = |x|$,

$$\begin{cases} \Delta^2 u - \kappa^4 u = 0 \quad \text{in } \mathbb{R}^2 \setminus \overline{D} \\ u = 0, \quad \partial_n u = 0 \quad \text{on } \partial D \\ \lim\limits_{r\to\infty} \sqrt{r}\,(\partial_r u^s - i\kappa u^s) = 0, \quad \lim\limits_{r\to\infty} \sqrt{r}\,(\partial_r \Delta u^s - i\kappa \Delta u^s) = 0\,(\mathit{SRC}) \end{cases} \tag{1}$$

Remark

Let $u^i = \exp(i\kappa x \cdot d)$ *then the radiating scattered field* $u^s(x, d; \kappa)$ *depends on the incident direction* d *and wave number* k.

Well-posedness of Direct Clamped Cavity Scattering Problem

The well-posedness of the direct clamped cavity scattering problem has been studied:

- Variational Method & Riesz-Fredholm theory
  Bourgeouis, L. and Hazard, C. (2020), On Well-Posedness of Scattering Problems in a Kirchhoff-Love Infinite Plate, SIAM Journal on Applied Mathematics 80(3), 1546-1556.
- Boundary Integral Equation Method & Riesz-Fredholm Theory
  Li, P. and Dong, H. (2024), A Novel Boundary Integral Formulation for the Biharmonic Wave Scattering Problem, Journal of Scientific Computing 98(42), 1-29.

Inverse Clamped Cavity Problem

The outgoing scattered field, also known as the radiating solution, satisfies

$$u^s(x) = \frac{e^{i\kappa r}}{\sqrt{r}} u^\infty(\hat{x}) + O\left(\frac{1}{r^{3/2}}\right) \quad \text{as } r = |x| \to \infty, \quad \hat{x} = x/r$$

$u^\infty(\hat{x}) : \mathbb{S}^1 \to \mathbb{C}$ defined on the unit sphere is called the far-field pattern.
Now define the far-field operator as

Definition (Far-Field Operator (aka Relative Scattering Operator))

$$\mathcal{F} : L^2(\mathbb{S}^1) \to L^2(\mathbb{S}^1), \quad (\mathcal{F}g)(\hat{x}) = \int_{\mathbb{S}^1} u^\infty(\hat{x}, d) g(d)\, ds(d).$$

$\mathcal{F}g = u_g^\infty$, where u_g^∞ is the far-field pattern of the scattered field u_g^s with incident wave $v_g(x) := \int_{\mathbb{S}^1} g(d) e^{i\kappa x \cdot d}\, ds(d)$ (Hergotz wave function)

Inverse clamped cavity problem: Given $\mathcal{F}$ for a range of wave numbers κ obtain qualitative information about the clamped cavity D in a thin elastic plate.

Biharmonic Wave Decomposition

Consider the two auxiliary functions

$$u_H^s = -\frac{1}{2\kappa^2}(\Delta u^s - \kappa^2 u^s), \quad u_M^s = \frac{1}{2\kappa^2}(\Delta u^s + \kappa^2 u^s)$$

u_H^s is the **Helmholtz component** of u^s and u_M^s is the **modified Helmholtz component** of u^s such that

$$u^s = u_H^s + u_M^s, \quad \Delta u^s = \kappa^2(u_M^s - u_H^s)$$

u_H^s and u_M^s satisfy the Helmholtz equation and modified Helmholtz equation respectively

$$\Delta u_H^s + \kappa^2 u_H^s = 0, \quad \Delta u_M^s - \kappa^2 u_M^s = 0 \quad \text{in } \mathbb{R}^2 \setminus \overline{D}$$

Biharmonic Wave Decomposition

We can reformulate the scattering problem (1) as

$$\begin{cases} \Delta u_H^s + \kappa^2 u_H^s = 0, \quad \Delta u_M^s - \kappa^2 u_M^s = 0 \quad \text{in } \mathbb{R}^2 \setminus \overline{D} \\ u_H^s + u_M^s = -u^i, \quad \partial_n u_H^s + \partial_n u_M^s = -\partial_n u^i \quad \text{on } \partial D \\ \lim\limits_{r\to\infty} \sqrt{r}\,(\partial_r u_H^s - i\kappa u_H^s) = 0 \\ \lim\limits_{r\to\infty} \sqrt{r}\,(\partial_r u_M^s - i\kappa u_M^s) = 0, \quad r = |x| \end{cases} \tag{2}$$

Biharmonic Wave Decomposition

We can reformulate the scattering problem (1) as

$$\begin{cases} \Delta u_H^s + \kappa^2 u_H^s = 0, \quad \Delta u_M^s - \kappa^2 u_M^s = 0 \quad \text{in } \mathbb{R}^2 \setminus \overline{D} \\ u_H^s + u_M^s = -u^i, \quad \partial_n u_H^s + \partial_n u_M^s = -\partial_n u^i \quad \text{on } \partial D \\ \lim\limits_{r\to\infty} \sqrt{r}\,(\partial_r u_H^s - i\kappa u_H^s) = 0 \\ \lim\limits_{r\to\infty} \sqrt{r}\,(\partial_r u_M^s - i\kappa u_M^s) = 0, \quad r = |x| \end{cases} \tag{2}$$

Remark (Exponential Decay of u_M^s)

u_M^s and $\partial_r u_M^s$ exhibit exponential decay as $r = |x| \to \infty$ for the fixed wavenumber κ as $\kappa r \to \infty$. Specifically, u_M^s satisfies

$$u_M^s(x) = O\left(\frac{e^{-kr}}{\sqrt{r}}\right), \; r \to \infty$$

Far-Field Pattern of the Biharmonic Scattered Field

Because of the exponential decay of the evanescent part u^s_M and $\partial_n u^s_M$, the far-field pattern contains only information about the Helmholtz component, thus,

$$u^\infty(\hat{x}) = u^\infty_H(\hat{x}),$$

up to a constant depending on κ. By Rellich's lemma and exp. decay of u^s_M, we obtain

Lemma (P.Li & H.Dong, 2023)

if $u^s \in C^4(\mathbb{R}^2 \setminus \overline{D})$ *satisfies*

$$\lim_{r\to\infty} \int_{|x|=r} |u^s(x)|^2 \, ds = 0,$$

then $u^s_H = 0$ *in* $\mathbb{R}^2 \setminus \overline{D}$. *Thus,*

$$u^\infty = 0 \implies u^s_H = 0 \text{ in } \mathbb{R}^2 \setminus \overline{D}.$$

Reconstruction Methods

1. Iterative methods to determine D (expensive optimization; a good initial guess is needed; only one or a few incident waves are needed; reconstructions are reasonably good)
2. Domain decomposition methods (solve an ill-posed linear integral equation first to reduce computational expense, then optimize)
3. **Direct imaging methods** (avoid optimization entirely, solve many ill-posed integral equations, requires a lot of multistatic data but **no a priori information**; partial qualitative information about the scatterer is obtained)

Reconstruction of D via Direct Imaging Methods

Remark (Shape Reconstruction)

Direct Imaging Methods: *the idea is to construct an indicator test function I that will test whether a point z lies inside or outside the scatterer.*
Benefits: *can reconstruct the shape of the scatterer in a computational simple manner with* **no a priori information***.*

- Assume only the location and shape of the object is needed (e.g., looking for a crack or cavity).
- Based on model, derive an indicator test function $I(z)$, depending on coordinates, so that

$$I(z) = \begin{cases} 0, & z \notin \text{ object} \\ 1, & z \in \text{ object} \end{cases}$$

- $I(z)$ must be fast to compute from the scattered or far-field data.

Categorizing Direct Imaging Methods

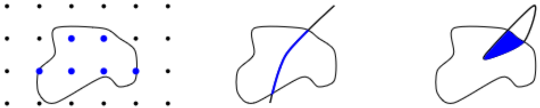

Figure: Approaches to Qualitative Imaging

- ‘96 Colton – Kirsch: linear sampling method, factorization (point sampling in grid)
- ‘98 Ikehata: probing method (curve); ‘00 Potthast: singular source method (curve/needle)
- ... Luke, Potthast, Sylvester, Kusiak, Ikehata: range test, no response test, enclosure method (sets/planes)

Results on Inverse Shape Problem for Biharmonic Plate Equation

- L. Bourgeouis & A. Recoquillay (2020): recovery of clamped cavities and cavities in a free plate with the linear sampling method with near-field measurements (boundary measurements)
  Disadvantage: uses far more multistatic data, namely scattered field and normal derivative of scattered field for point source and dipole
- Y. Chang & Y. Guo (2023): recovery of clamped cavities in a thin elastic plate with near field measurements via the domain decomposition method (optimization method)
- I. Harris, P. Li, & H. Lee (2024): recovery and resolution analysis of clamped cavities with the direct sampling method
- A. Karageorghis & D. Lesnic (2024): method of fundamental solutions (iterative method) for recovering clamped and free plate cavities with near field measurements

Uniqueness Result

Theorem (P. Li & H. Dong, 2023)

Let D_1 and D_2 be two cavities meeting the clamped boundary conditions, with corresponding far-field patterns u_1^∞ and u_2^∞ satisfying

$$u_1^\infty(\hat{x}, d) = u_2^\infty(\hat{x}, d), \quad \forall \hat{x}, d \in \mathbb{S}^1.$$

Then $D_1 = D_2$.

- This result guarantees uniqueness of the inverse cavity scattering problem with clamped boundary conditions.
- Proof of the result is based on the reciprocity relations and correspondences of the far-field patterns with respective scattered fields generated by point sources.

Idea Behind Linear Sampling Method

Qualitative/Sampling Scheme
Goal: want to

- recover shape and location of the cavity using an indicator function based on an integral equation solution

Sampling: Collect the far-field data u^∞ and solve an ill-posed linear integral equation for each sample point z

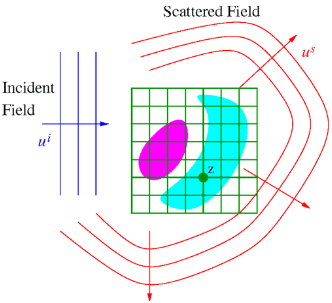

Core of LSM - The Far-Field Equation

Far-Field Equation

$$\mathcal{F}g_z(\hat{x}) = \Phi^\infty(\hat{x}, z), \quad \Phi^\infty(\hat{x}, z) = -\frac{1}{2\kappa^2}\frac{e^{i\pi/4}}{\sqrt{8\kappa\pi}}e^{-i\kappa x\cdot z}, \; g_z \in L^2(\mathbb{S}^1), \; z \in \mathbb{R}^2$$

- $\Phi^\infty(\cdot, z) =$ FF pattern of the point source $\Phi(\cdot, z)$ centered at sampling point z
- $\Phi(\cdot, z)$ satisfies $(\Delta^2 - \kappa^4)\Phi(\cdot, z) = (\Delta - \kappa^2)(\Delta + \kappa^2)\Phi(\cdot, z) = -\delta(\cdot - z)$ in $\mathbb{R}^2$ with

$$\begin{aligned}\Phi(x, z) &= \frac{i}{8\kappa^2}\left(H_0^1(\kappa|x-z|) + \frac{2i}{\pi}K_0(\kappa|x-z|)\right), \quad x \neq z \\ &= \frac{1}{2\kappa^2}(\Phi_H(x, z) - \Phi_M(x, z)),\end{aligned}$$

  where $H_0^{(1)}$ and K_0 are the Hankel functions of the first kind and MacDonald's function, respectively.
- $\mathcal{F}$ is a compact operator, so the FF equation is **ill-posed**.

Approximate Solvability Condition of Far-Field Equation

Want an **approximate solvability condition** for the FF equation:

Problem

Approximate Solvability Condition: *want to show $\mathcal{F}$ has dense range in $L^2(\mathbb{S}^1)$; that is,*

$$\overline{\textit{Range } \mathcal{F}}^{||\cdot||_{L^2(\mathbb{S}^1)}} = L^2(\mathbb{S}^1)$$

By Hahn-Banach Theorem, this is equivalent to showing the adjoint operator $\mathcal{F}^*$ is injective. By a result called the **reciprocity relation**, the approximate solvability condition reduces to showing $\mathcal{F}$ is injective.

Approximate Solvability and Reciprocity Relation

Lemma (Reciprocity Relation)

$u^\infty(\hat{x}, d) = u^\infty(-d, -\hat{x})$ *for every* $\hat{x}, d \in \mathbb{S}^1$.

Proof uses Green's representation formula for u^∞ + exploits exp. decay of u_M^s. **Why is this useful?**

$$
\begin{aligned}
(f, \mathcal{F}g)_{L^2(\mathbb{S}^1)} &= \int_{\mathbb{S}^1} \left(\overline{\int_{\mathbb{S}^1} u^\infty(\hat{x}, d) g(d)\, ds(d)} \right) ds(\hat{x}) \\
&= \int_{\mathbb{S}^1} \left(\overline{\int_{\mathbb{S}^1} u^\infty(-d, -\hat{x}) g(d)\, ds(d)} \right) ds(\hat{x}) \\
&= \left(\overline{u^\infty(-d, -\hat{x})} f(\hat{x}) ds(\hat{x}), g \right)_{L^2(\mathbb{S}^1)},
\end{aligned}
$$

so $\mathcal{F}^* g = \overline{R\mathcal{F}R\overline{g}}$ where $(Rf)(\hat{x}) := f(-\hat{x})$.
Approximate Solvability: Suffices to show $\mathcal{F}$ is injective!

Assumption for Approximate Solvability

We want to determine when $\mathcal{F}$ is injective. Suppose $\mathcal{F}g = u_g^\infty = 0$. Then by Rellich's lemma + exp. decay of the modified Helmholtz component,

$$u_{g,H}^s(x) = \int_{\mathbb{S}^1} u_H^s(x,d)g(d)\,ds(d) = 0 \text{ in } \mathbb{R}^2 \setminus \overline{D},$$

with

$$\begin{aligned} \Delta u_{g,M}^s - \kappa^2 u_{g,M}^s &= 0 \text{ in } \mathbb{R}^2 \setminus \overline{D}, \\ \Delta u_{g,H}^s + \kappa^2 u_{g,H}^s &= 0 \text{ in } D, \end{aligned} \tag{3}$$

and so on the boundary ∂D:

$$u_{g,M}^s + v_g = 0, \quad \partial_n(u_{g,M}^s + v_g) = 0. \tag{4}$$

Assume: $\kappa^2 \neq$ eigenvalue of (3)–(4) to ensure $v_g = 0$ on ∂D, so that $g = 0$. (Only want trivial solution pair)

Helpful Auxiliary Operators for Approximate Solvability

Define the Herglotz wave operator

$$\mathcal{H} : L^2(\mathbb{S}^1) \to H^{3/2}(\partial D) \times H^{1/2}(\partial D) \; : \; g \mapsto \begin{pmatrix} v_g \\ \partial_n v_g \end{pmatrix}\Bigg|_{\partial D},$$

where $v_g(x) = \int_{\mathbb{S}^1} e^{i\kappa x \cdot d} g(d)\, ds(d)$ is the Herglotz wave function. Then

$$\boxed{\mathcal{F} = -\mathcal{G}\mathcal{H}}$$

- $\mathcal{G}$: boundary data $\mapsto$ FF pattern (data-to-pattern operator)
- $\mathcal{H}$ is the Herglotz wave operator that maps g to the superposition of plane wave data on the boundary.
- By superposition $\mathcal{H}g$ induces the far-field pattern $\mathcal{F}g$

On Auxiliary Operator $\mathcal{G}$

$\mathcal{G} : H^{3/2}(\partial D) \times H^{1/2}(\partial D) \to L^2(\mathbb{S}^1) : (h_1, h_2)^\top \mapsto w^\infty$

1. w^∞ = far-field pattern of the unique radiating solution $w \in H^2_{\text{loc}}(\mathbb{R}^2 \setminus \overline{D})$ satisfying

$$\begin{cases} \Delta^2 w - \kappa^4 w = 0 \quad \text{in } \mathbb{R}^2 \setminus \overline{D}, \\ w|_{\partial D} = h_1, \quad \partial_n w|_{\partial D} = h_2, \\ \lim\limits_{r=|x|\to\infty} \sqrt{r}\,(\partial_r w - i\kappa w) = 0, \lim\limits_{r=|x|\to\infty} \sqrt{r}\,(\partial_r \Delta w - i\kappa \Delta w) = 0 \end{cases} \tag{5}$$

2. To show $\mathcal{G}$ is injective, we need to assume that $\kappa^2 \neq$ eigenvalue of the mixed eigenvalue problem given by the pair $(p, q) = (w_M, u^i)$ satisfying

$$\begin{cases} \Delta p - \kappa^2 p = 0 \quad \text{in } \mathbb{R}^2 \setminus \overline{D}, \\ \Delta q + \kappa^2 q = 0 \quad \text{in } D, \\ p + q = 0, \quad \partial_n (p + q) = 0 \quad \text{on } \partial D, \\ \lim\limits_{r=|x|\to\infty} \sqrt{r}\,(\partial_r p - i\kappa p) = 0, \end{cases} \tag{6}$$

Approximate Solvability of the FF equation

The following two lemmas ensure the approximate solvability condition of the far-field equation holds:

Lemma (G. Ozochiawaeze, 2024)

The auxiliary operator $\mathcal{G}$ is compact with dense range on $L^2(\mathbb{S}^1)$. Moreover, if $\kappa^2 \neq$ eigenvalue of (6), then $\mathcal{G}$ is injective. Finally, we have the following range characterization of the clamped cavity D:

$$z \in D \iff \Phi^{\infty}(\hat{x}, z) \in \mathit{Range}(\mathcal{G}).$$

Lemma (G. Ozochiawaeze, 2024)

$\mathcal{H}$ is compact and injective. If $\kappa^2 \neq$ eigenvalue of (6), then $\mathcal{F}$ is injective. Thus, $\mathcal{F}$ has dense range in $L^2(\mathbb{S}^1)$.

Range Characterization of the Cavity D

The **linear sampling method** is a direct imaging method based on the following range characterization of the cavity D:

Lemma (Range Characterization of Clamped Cavity D)

$z \in D$ if and only if $\Phi^{\infty}(\hat{x}, z) \in$ Range$(\mathcal{G})$.

This result follows by Rellich's lemma and justifies the choice of indicator test function of LSM:

$$I(z) := \frac{1}{||g_z||_{L^2(\mathbb{S}^1)}} = \begin{cases} 0, & \text{if } z \in \mathbb{R}^2 \setminus D, \\ > 0, & \text{if } z \in D. \end{cases}$$

Moreover, $I(z) \to 0$ as $z \to \partial D$.

Reconstruction of the Cavity D via the LSM

Theorem (The Linear Sampling Method)

Assume $\kappa \neq$ eigenvalue of the mixed eigenvalue problem (6). We have the following:

- *Suppose $z \in D$. Given $\epsilon > 0$ there exists an approximate solution $g_{z,\epsilon} \in L^2(\mathbb{S}^1)$ to the far-field equation such that*

  $$||\mathcal{F}g_{z,\epsilon} - \Phi^{\infty}(\cdot, z)||_{L^2(\mathbb{S}^1)} < \epsilon.$$

  Furthermore, $||g_{z,\epsilon}||_{L^2(\mathbb{S}^1)}$ is **unbounded** *as $z \to \partial D$.*

- *Suppose $z \notin D$. Then the approximate solution of the far-field equation $g_{z,\epsilon}$ satisfies*

  $$||g_{z,\epsilon}||_{L^2(\mathbb{S}^1)} \text{ is } \textbf{unbounded} \text{ as } \epsilon \to 0, \text{ assuming that}$$

  $$||\mathcal{F}g_{z,\epsilon} - \Phi^{\infty}(\cdot, z)||_{L^2(\mathbb{S}^1)} \to 0 \quad \text{as } \epsilon \to 0.$$

Numerical Scheme

- Construct a grid of 'sampling points' $\mathcal{T}$ in a region known to contain the cavity D. Choose a regularization parameter $\alpha > 0$ and cut-off constant c_0.
- For each grid point $z_i \in \mathcal{T}$, solve the regularized far-field equation $(\alpha I + \mathcal{F}^*\mathcal{F})g_{z_i,\alpha} = \mathcal{F}^*\Phi^\infty(\hat{x}, z_i)$ (Tikhonov regularization)
- Construct a reconstruction M for D where

$$M := \{z_i \in \mathcal{T} \,:\, ||g_{z_i,\alpha}||_{L^2(\mathbb{S}^1)} \leq c_0\}$$

Choice of c_0 is heuristic; resolution improves with higher wave number. If we invert the indicator function, $c_0 = 0$.

Numerical Result: Recovering the Apple-Shaped Cavity

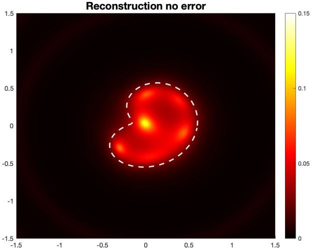

Figure: Recovering the Apple-Shaped Cavity with $\kappa = 2\pi$; no noise; 30 incident and observation directions; 250×250 grid

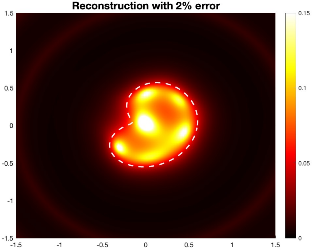

Figure: Recovering the Apple-Shaped Cavity with $\kappa = 2\pi$; noise $\delta = 0.02$; 30 incident and observation directions; 250×250 grid

Numerical Result: Recovering the Peach-Shaped Cavity

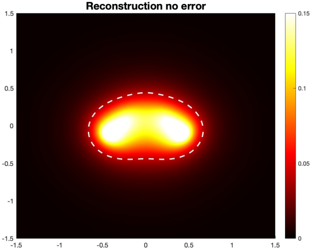

Figure: Recovering the Peach-Shaped Cavity with $\kappa = \pi$; no noise; 30 incident and observation directions; 250×250 grid

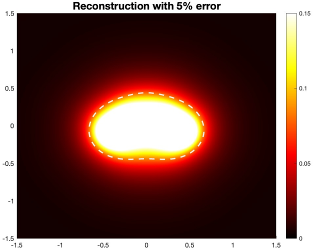

Figure: Recovering the Peach-Shaped Cavity with $\kappa = \pi$; noise $\delta = 0.05$; 30 incident and observation directions; 250×250 grid

Numerical Result: Recovering the Peanut-Shaped Cavity

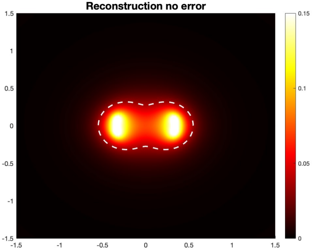

Figure: Recovering the Peanut-Shaped Cavity with $\kappa = \pi$; no noise; 30 incident and observation directions; 250×250 grid

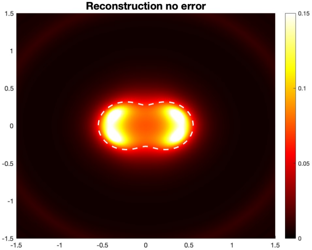

Figure: Recovering the Peanut-Shaped Cavity with $\kappa = 2\pi$; no noise; 30 incident and observation directions; 250×250 grid

Numerical Result: Recovering the Peanut-Shaped Cavity

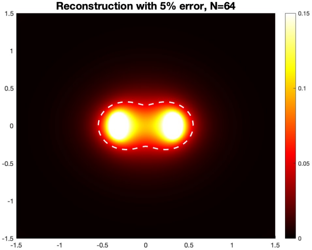

Figure: Recovering the Peanut-Shaped Cavity with $\kappa = \pi$; noise $\delta = 0.05$; 64 incident and observation directions; 250×250 grid

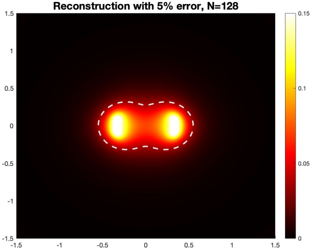

Figure: Recovering the Peanut-Shaped Cavity with $\kappa = \pi$; noise $\delta = 0.05$; 128 incident and observation directions; 250×250 grid

Ongoing Future Work

- numerical implementation of the linear sampling method for other cavities (e.g., free plate, simply supported plate, roller supported) based on Neumann and mixed boundary conditions with far-field data
- modification of the LSM for reconstructing cavities with a single incident plane wave (single measurement) (i.e., will consider the extended sampling method)